

Modeling of the high-energy galactic cosmic-ray anisotropy

M. Amenomori and The Tibet AS γ Collaboration

Department of Physics, Hirosaki University, Hirosaki 036-8561, Japan

Received: 16 October 2010 – Accepted: 16 November 2010 – Published: 9 December 2010

Abstract. A possible origin of the large-scale anisotropy of galactic cosmic rays at TeV energies is discussed. It can be well modeled by a superposition of the Global Anisotropy and the Midscale Anisotropy. The Global Anisotropy would be generated by galactic cosmic rays interacting with the magnetic field in the local interstellar space of scale ~ 2 pc surrounding the heliosphere. On the other hand, the Midscale Anisotropy, possibly caused by the modulation of galactic cosmic rays in the heliotail, is expressed as two intensity enhancements placed along the Hydrogen Deflection Plane, each symmetrically centered away from the heliotail direction. We find that the separation angle between the heliotail direction and each enhancement monotonously decreases with increasing energy in an energy range 4–30 TeV.

1 Introduction

Past cosmic-ray experiments consistently reported a cosmic-ray anisotropy in the sidereal time frame with an amplitude of $\sim 0.1\%$, suggesting that there are two distinct broad structures in the anisotropy; one is a deficit in the cosmic-ray flux (called the “loss-cone”), distributed around 150° to 240° in Right Ascension; the other is an excess in the cosmic-ray flux (called the “tail-in”), distributed around 40° to 90° in Right Ascension. Recent underground muon and air-shower experiments including the Tibet air-shower experiment studied the anisotropy in a great detail at multi-TeV energies (Amenomori et al., 2006; Guillian et al., 2007; Abbasi et al., 2009). The observed anisotropy of galactic cosmic rays at TeV energies is considered to reflect the structure of the local interstellar magnetic field surrounding the heliosphere, since the trajectories of charged cosmic rays are deflected

and scrambled by the local interstellar magnetic field while traveling through the interstellar medium.

2 Analysis and results

The Tibet air-shower array, located at 90.522° E, 30.102° N and 4300 m above sea level, has been operating successfully since 1990. In this paper, we analyze air-shower events collected during the period from November 1999 through December 2008 (1916 live days). After our standard data selection, 4.5×10^{10} events are left with a modal energy of 7 TeV. For more detail of the experiment and our analysis method, refer to our separate papers (Amenomori et al., 2006, 2007; Munakata et al., 2009). We include in the systematic error the amplitude observed in the anti-sidereal time frame (364.2422 cycles/yr), because a possible seasonal change of the solar daily variation due to solar activities might produce a spurious variation in the sidereal time frame, which can be estimated by the daily variation observed in the anti-sidereal time frame. We calculate the root mean square of the anti-sidereal anisotropy in each declination band, and add it as the systematic error to the statistical error for the sidereal anisotropy in the corresponding declination band. Figure 1a shows the obtained relative intensity in $5^\circ \times 5^\circ$ pixels. We model this observed anisotropy in terms of two components as (Munakata et al., 2009):

$$I_{n,m} = I_{n,m}^{GA} + I_{n,m}^{MA}, \quad (1)$$

where $I_{n,m}^{GA}$ and $I_{n,m}^{MA}$ denote the intensity of the Global Anisotropy (GA) and the Midscale Anisotropy (MA) of the (n, m) pixel in the equatorial coordinate system, respectively. The $I_{n,m}^{GA}$ is further expressed as the combination of an unidirectional flow (UDF) and a bi-directional flow (BDF):

$$I_{n,m}^{GA} = a_{1\perp} \cos \chi_1(n, m : \alpha_1, \delta_1) + a_{1\parallel} \cos \chi_2(n, m : \alpha_2, \delta_2) + a_{2\parallel} \cos^2 \chi_2(n, m : \alpha_2, \delta_2). \quad (2)$$



Correspondence to: T. K. Sako
(tsako@icrr.u-tokyo.ac.jp)

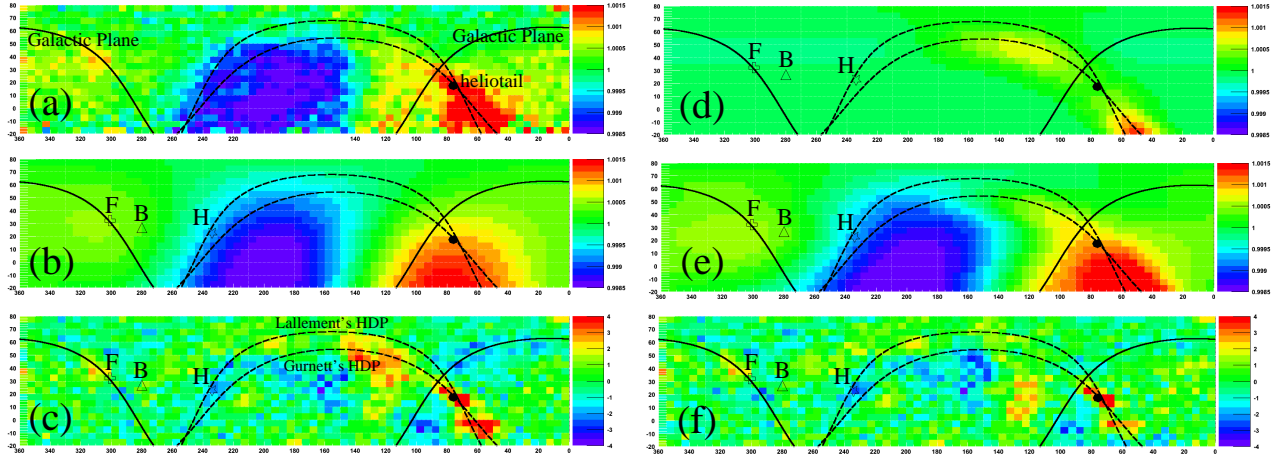


Fig. 1. 2D anisotropy maps of galactic cosmic rays observed and reproduced at the modal energy of 7 TeV. Each map shows the relative intensity or the significance in $5^\circ \times 5^\circ$ pixels in the equatorial coordinate system.

(a): the observed cosmic-ray intensity ($I_{n,m}^{obs}$), (b): the best-fit Global Anisotropy (GA) component ($I_{n,m}^{GA}$), (c): the significance map of the residual anisotropy after subtracting $I_{n,m}^{GA}$ from $I_{n,m}^{obs}$, (d): the best-fit Midscale Anisotropy (MA) component ($I_{n,m}^{MA}$), (e): the best-fit GA+MA components ($I_{n,m}^{GA} + I_{n,m}^{MA}$), and (f): the significance map of the residual anisotropy after subtracting $I_{n,m}^{GA} + I_{n,m}^{MA}$ from $I_{n,m}^{obs}$.

The solid black curves represent the galactic plane. The dashed black curves represent the Hydrogen Deflection Plane reported by Gurnett et al. (Gurnett et al. (2006)) and Lallement et al. (Lallement et al. (2005)). The heliotail direction (α, δ) = (75.9°, 17.4°) is indicated by the black filled circle. The open cross and the inverted star with the attached characters “F” and “H” represent the orientation of the local interstellar magnetic field (LISMF) by Frisch (1996) and Heerikhuisen et al. (2010), respectively. The open triangle with “B” indicates the orientation of the best-fit bi-directional cosmic-ray flow (BDF) obtained in this paper.

In Eq. (2), (α_2, δ_2) denotes the orientation of the reference axis of the BDF, and $a_{2\parallel}$ the amplitude of the BDF. The UDF is decomposed into two components; one is parallel to the BDF with an amplitude of $a_{1\parallel}$, and the other is perpendicular with an amplitude of $a_{1\perp}$ along the orientation of the reference axis (α_1, δ_1) perpendicular to (α_2, δ_2) . The χ_1 denotes the angular distance of the center of the (n, m) pixel measured from the reference axis (α_1, δ_1) , and χ_2 denotes that measured from the axis (α_2, δ_2) . Figure 1b shows the reproduced anisotropy when we attempt to fit Fig. 1a with $I_{n,m}^{GA}$ alone. Although Fig. 1b successfully reproduces the global “tail-in” and “loss-cone” structures, there remains the midscale anisotropy, as can be seen in Fig. 1c. The $I_{n,m}^{MA}$, incorporated to model this residual excess of intensity, is expressed as:

$$I_{n,m}^{MA} = \left\{ b_1 \exp\left(-\frac{(\phi_{n,m} - \Phi)^2}{2\sigma_\phi^2}\right) + b_2 \exp\left(-\frac{(\phi_{n,m} + \Phi)^2}{2\sigma_\phi^2}\right) \right\} \times \exp\left(-\frac{\theta_{n,m}^2}{2\sigma_\theta^2}\right), \quad (3)$$

where b_1 and b_2 denote the amplitudes of the two excess components along the best-fit plane with the heliotail direction on it, each centered away from the heliotail direction by an angle Φ along the plane. The σ_ϕ (σ_θ) denotes the width of the excess parallel (perpendicular) to the best-fit plane, $\phi_{n,m}$ and $\theta_{n,m}$ the “longitude” measured from the heliotail

direction and the “latitude” of the center of the (n, m) pixel measured from the best-fit plane. Figure 1e and f show the reproduced anisotropy and the residual anisotropy when we fit Fig. 1a with $I_{n,m}^{GA} + I_{n,m}^{MA}$. The $I_{n,m}^{MA}$ extracted from Fig. 1e is shown in Fig. 1d. Note that the obtained best-fit plane along which the MA is assumed is fairly consistent with the Hydrogen Deflection Plane (HDP) suggested by Gurnett et al. (2006), which contains the directions of the interstellar wind velocity and the interstellar magnetic field upstream the helionose; the angle difference between the direction normal to our best-fit plane and that to Gurnett’s HDP is only 2.1°. The best-fit parameters in Eq. (2) and Eq. (3) are listed in Table 1.

3 Discussions

The GA can be interpreted as follows (for details, see Munakata et al., 2009; Mizoguchi et al., 2009). The local interstellar space of scale ~ 2 pc surrounding the heliosphere would be responsible for the GA. The BDF is produced by cosmic rays drifting parallel to the Local Interstellar Magnetic Field (LISMF) line into the heliosphere from outside the Local Interstellar Cloud surrounding the heliosphere. The UDF, perpendicular to the LISMF ($a_{1\perp} \gg a_{1\parallel}$) with its amplitude comparable to that of the BDF ($a_{1\perp} \simeq a_{2\parallel}$), can be produced by a diamagnetic drift arising from a spatial density gradient ($\nabla n/n$) of galactic cosmic rays in the LISMF.

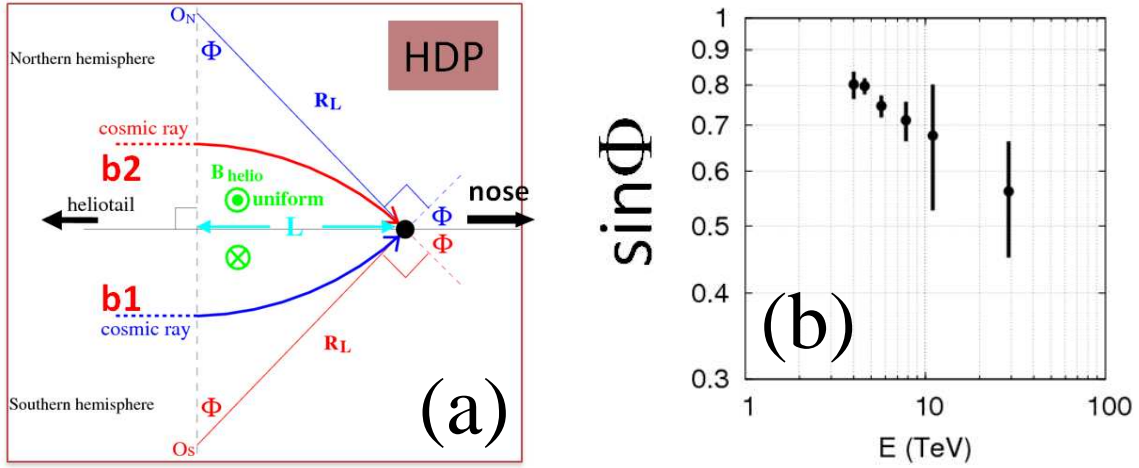


Fig. 2. (a): a possible mechanism for the Midscale Anisotropy. (b): the observed energy dependence of $\sin\Phi$.

Table 1. Best-fit parameters in Eq. (2) and Eq. (3) for the 2D galactic-cosmic-ray anisotropy map observed at 7 TeV.

Global Anisotropy (GA)						
$a_{1\perp}$ (%)	$a_{1\parallel}$ (%)	$a_{2\parallel}$ (%)	α_1 (°)	δ_1 (°)	α_2 (°)	δ_2 (°)
0.139 ± 0.002	0.007 ± 0.002	0.131 ± 0.004	33.3 ± 1.1	38.4 ± 1.2	279.9 ± 0.9	-26.7 ± 2.0
Mid-scale Anisotropy (MA)						
b_1 (%)	b_2 (%)	σ_ϕ (°)	σ_θ (°)	Φ (°)		
0.154 ± 0.018	0.092 ± 0.006	24.5 ± 1.1	10.7 ± 0.8	49.2 ± 1.4		

A sketch of a possible mechanism for the MA is shown in Fig. 2a. The orientation of the magnetic field in the heliotail B_{helio} is toward (away from) the Sun in the northern (southern) hemisphere during the period we analyzed. Let us assume, for simplicity, that the B_{helio} surrounding the solar system is uniform within the spatial scale L toward the heliotail direction. Then, the uniform B_{helio} bends the trajectories of cosmic rays propagating along the HDP from the heliotail direction, leading them to the solar system. A simple geometrical consideration gives the following relation:

$$\begin{aligned} L [\text{AU}] &= R_L [\text{AU}] \sin\Phi \\ &= 206(E [\text{TeV}]/B_{\text{helio}} [\mu\text{G}])\sin\Phi, \end{aligned} \quad (4)$$

where R_L is the Larmor radius of cosmic rays with energy E in B_{helio} . This equation implies $\sin\Phi \propto 1/E$ if L is independent of energy. The observed energy dependence of $\sin\Phi$, shown in Fig. 2b, gives the following function:

$$\sin\Phi = (0.68 \pm 0.04) (E/10 [\text{TeV}])^{-0.20 \pm 0.08}, \quad (5)$$

suggesting $L \propto E^{0.8}$. This energy dependence of L might result from actual complex spatial structures of B_{helio} , which could be identified in the future by studying the cosmic-ray transport in B_{helio} by means of Magneto-Hydrodynamic sim-

ulations (Washimi et al., 2007). Substituting Eq. (5) into Eq. (4) and assuming $B_{\text{helio}} = 10 \mu\text{G}$, we get

$$L [\text{AU}] = (140 \pm 8) (E/10 [\text{TeV}])^{0.80 \pm 0.08}, \quad (6)$$

implying that B_{helio} within ~ 70 AU to ~ 340 AU from the Sun is responsible for the MA, in the energy range of 4–30 TeV. The MA being placed along the HDP suggests that it is possibly caused by the modulation of galactic cosmic rays in B_{helio} . Another candidate for the heliospheric signature might be the excess region first reported as the “hot-spot” by the Milagro experiment (Abdo et al. (2008)). This region corresponds to the pixel in Fig. 1a centered at $(72.5^\circ, 17.5^\circ)$, close to the heliotail, observed with the highest significance 9.06σ among all the pixels. It is difficult to interpret such a collimated excess as a cosmic-ray inflow along the neutral sheet that separates B_{helio} between the northern and southern hemispheres. The Milagro experiment reported that the “hot-spot” has a localized spatial extension with a half-width of $2.6^\circ \pm 0.3^\circ$ and a half-length of $7.6^\circ \pm 1.1^\circ$. We need to note here that the size of such a small-scale structure is greatly susceptible to the size and shape of the analysis window for background estimation to subtract the large-scale anisotropy superposed on the structure.

4 Conclusions

We discussed the origin of the large-scale anisotropy of galactic cosmic rays at TeV energies. It can be well modeled by a superposition of the Global Anisotropy and the Midscale Anisotropy.

The GA, for which the local interstellar space of scale ~ 2 pc surrounding the heliosphere would be responsible, is expressed as the combination of a UDF and a BDF of galactic cosmic rays. The BDF is produced by cosmic rays drifting parallel to the LISMF line into the heliosphere from outside the Local Interstellar Cloud surrounding the heliosphere. Meanwhile, the UDF, which is perpendicular to the LISMF, can be produced by a diamagnetic drift arising from a spatial density gradient of galactic cosmic rays in the LISMF.

The MA, for which B_{helio} within ~ 70 AU to ~ 340 AU from the Sun is responsible in the energy range of 4–30 TeV, is expressed as two cosmic-ray intensity enhancements placed along the HDP and symmetrically centered away from the heliotail direction, with the separation angle between the heliotail direction and each of the two enhancements decreasing monotonously with increasing energy in the energy range of 4–30 TeV. The MA being placed along the HDP, which contains the directions of the interstellar wind velocity and the interstellar magnetic field surrounding the heliosphere, suggests that it is possibly caused by the modulation of galactic cosmic rays in the magnetic field of the heliotail.

Supplementary material related to this article is available online at:
<http://www.astrophys-space-sci-trans.net/6/49/2010/astra-6-49-2010-supplement.supplement.pdf>.

Acknowledgements. The collaborative experiment of the Tibet Air Shower Arrays has been performed under the auspices of the Ministry of Science and Technology of China and the Ministry of Foreign Affairs of Japan. This work was supported in part by a Grant-in-Aid for Scientific Research on Priority Areas from the Ministry of Education, Culture, Sports, Science and Technology, by Grants-in-Aid for Science Research from the Japan Society for the Promotion of Science in Japan, and by the Grants from the National Natural Science Foundation of China and the Chinese Academy of Sciences.

Edited by: B. Heber

Reviewed by: two anonymous referees

References

- Abbasi, R. U., Velez, J. C., and Desiati, P. for the IceCube Collaboration: Large Scale Cosmic Rays Anisotropy With IceCube, arXiv:0907.0498, 2009.
- Abdo, A. A. for Milagro Collaboration: Discovery of Localized Regions of Excess 10-TeV Cosmic Rays, *Phys. Rev. Lett.*, 101, 221 101–221 105, 2008.
- Amenomori, M., Ayabe, S., Bi, X. J. et al.: Implication of the sidereal anisotropy of 5 TeV cosmic ray intensity observed with the Tibet III air shower array, *AIP Conf. Proc.*, 932, 283–289, 2007.
- Amenomori, M., Ayabe, S., Bi, X. J. et al.: Anisotropy and Corotation of Galactic Cosmic Rays, *Science*, 314, 439–443, 2006.
- Amenomori, M., Bi, X. J., Chen, D., et al.: Large-scale sidereal anisotropy of multi-TeV galactic cosmic rays and the heliosphere, arXiv:0909.1026, 2009.
- Frisch, P. C.: LISM structure - Fragmented superbubble shell?, *Space Sci. Rev.*, 78, 213–222, 1996.
- Guillian, G., Hosaka, J., Ishihara, K., et al.: Observation of the anisotropy of 10 TeV primary cosmic ray nuclei flux with the Super-Kamiokande-I detector, *Phys. Rev. D*, 75, 062 003–062 019, 2007.
- Gurnett, D. A., Kurth, W. S., Cairns, I. H., et al.: The local interstellar magnetic field direction from direction-finding measurements of heliospheric 2–3 kHz radio emissions, *AIP Conf. Proc.*, 858, 129–134, 2006.
- Heerikhuisen, J., Pogorelov, N. V., Zank, G. P., et al.: Pick-Up Ions in the Outer Heliosheath: A Possible Mechanism for the Interstellar Boundary EXplorer Ribbon, *Astrophys. J. Lett.*, 708, L126–L130, 2010.
- Lallement, R., Quémerais, E., Bertaux, J. L., et al.: Deflection of the Interstellar Neutral Hydrogen Flow Across the Heliospheric Interface, *Science*, 307, 1447–1449, 2005.
- Mizoguchi, Y., Munakata, K., Takita, M., et al.: The sidereal anisotropy of multi-TeV cosmic rays in an expanding Local Interstellar Cloud, arXiv:0909.1029, 2009.
- Washimi, H., Zank, G. P., Hu, Q., et al.: A Forecast of the Heliospheric Termination-Shock Position by Three-dimensional MHD Simulations, *Astrophys. J. Lett.*, 670, L139–L142, 2007.